The final publication is available at

http://doi.org/10.1109/LAWP.2017.2767182

Additional Information

Low-profile Radially Corrugated Horn Antenna

Hon Ching Moy-Li, Daniel Sánchez-Escuderos, *Member, IEEE,*

Eva Antonino-Daviu, *Member, IEEE,* Miguel Ferrando-Bataller, *Member, IEEE,*

Abstract—This letter proposes a low-profile horn antenna with radial corrugations. The depth and width of the corrugations are suitably chosen to excite the mode HE_{11} in the corrugated section. This mode spreads uniformly across the whole aperture, thereby maximizing the radiating area and the aperture efficiency. The good polarization purity of mode HE_{11} provides a good cross-polar level and a low side-lobe level. The structure is fed by a circular waveguide with two matching elements on the feeding plane that minimize the return loss level. A prototype has been fabricated and measured to operate in the K_u band. The prototype, with a height of just 6.9 mm, i.e., $0.3\lambda_0$, provides a maximum gain above 12.2 dBi and an aperture efficiency better than 72% within the operating frequency band.

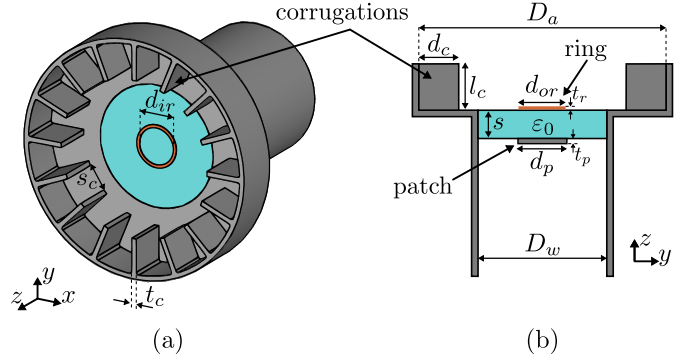*Index Terms*—Reflector antenna feeds, satellite antennas, corrugated horn antenna, hard surfaces.

Fig. 1. Proposed radially-corrugated circular horn antenna: (a) 3D model, and (b) inner view of a longitudinal section.

I. INTRODUCTION

CONICAL horn antennas are commonly used in space applications to feed reflector antennas. The position of the different horns depends on the desired coverage, e.g. multibeam [1] or contoured [2] but, in general, the distance between feeders must be kept small, which limits the apertures size. In addition, the illumination taper must be suitably chosen to compensate the spill-over and illumination efficiencies. For typical f/D ratios [1], the required illumination taper can only be achieved by means of a high aperture efficiency, given by a uniform amplitude and phase distribution on the aperture. To this aim, different types of horn antennas have been proposed during the last decades. These horns may be classified as multimode horns [3], hybrid horns [4] and hard horns [5].

Multimode horn antennas overlap two, or more, circular waveguide modes to extend the excited area beyond the fundamental TE_{11} mode pattern. The most representative example of this type of antennas is the Potter horn [6], which properly combines in phase modes TM_{11} and TE_{11} at the circular aperture. As a result, a considerably large aperture size is achieved, which gives a nearly symmetric co-polar pattern with a low level of cross-polarization.

Hybrid, or corrugated, horns [7] are aimed at exciting the hybrid HE_{11} mode, which is capable of extending the illuminated area across the whole circular aperture. The excitation of mode HE_{11} is given by means of transverse corrugations with a depth ranging between $\lambda/2$ and $\lambda/4$ along the conical horn path. The balanced hybrid condition given by mode

HE_{11} produces a symmetric radiation pattern with a low cross-polarization and low side lobes.

Hard horns use metamaterials on the lateral walls of the structures to maximize the aperture efficiency of the antenna [5]. Typically, metamaterials are formed by means of corrugations that create a high impedance surface on laterals. This high impedance prevents the longitudinal component of the electric field to cancel on walls, thereby obtaining a mode pattern similar to a balanced hybrid HE_{11} mode.

Previously-described horn antennas show a low cross-polar level and a high efficiency. However, the long centerline distance from the feeding waveguide to the aperture leads to high profile structures. In this letter, we propose an alternative solution aimed at reducing the length of the horn while keeping a good radiation performance.

The proposed horn antenna is a hard horn solution formed by a circular waveguide with radial corrugations. A proper configuration of the corrugations allows the excitation of mode HE_{11} in the waveguide, thereby maximizing the effective aperture size. The proposal follows the design presented in [8] but, now, a metal ring is additionally inserted to improve the cross-polar level. The resulting structure is 7 times smaller than multimode horns [6], and 26 shorter than conventional hybrid horn solutions [7]. A prototype has been fabricated and measured to validate the proposal.

II. RADIALLY CORRUGATED WAVEGUIDE

Fig. 1 shows a scketch of the proposed radially corrugated horn antenna (RCHA). The structure is formed by a circular waveguide (CW) with diameter D_w that feeds a radially corrugated waveguide (RCW) with diameter D_a opened to the free space. In the interface, two resonant elements, a metallic ring and a metallic circular patch, are inserted for matching purposes.
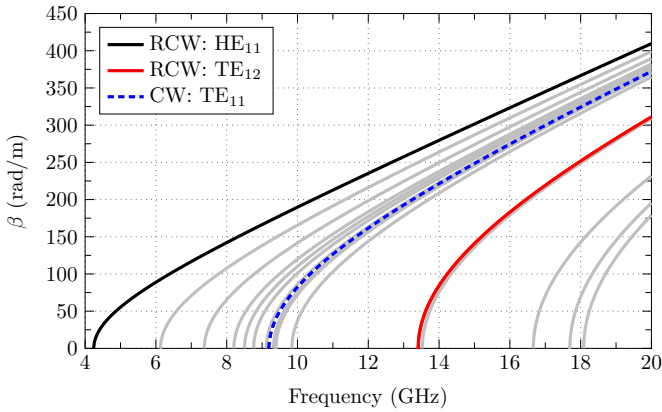
Fig. 2. Dispersion diagram of the radially corrugated waveguide (RCW), and propagation coefficient of the fundamental mode of the circular waveguide (CW).
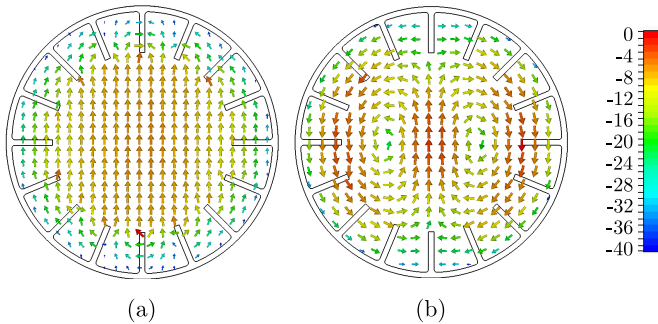

Fig. 3. Radially corrugated waveguide mode pattern: (a) Mode HE_{11}, and (b) Mode TE_{12}.

Corrugations of the RCW impose a hard surface condition on walls to allow the propagation of the hybrid mode HE_{11}. To this aim, the depth of the corrugations d_c is set to $\lambda/4$ [9], whereas the separation between corrugations s_c and the width of the corrugations t_c are chosen according to the following property [10]:

$$s_c \ll t_c + s_c \ll \lambda/2\sqrt{\varepsilon_r}. \tag{1}$$

In order to have an aperture size of 1.5λ at the lowest operating frequency (12 GHz), a diameter D_a=37.27 mm is chosen. Considering the central operating frequency for the design of the corrugations (12.75 GHz), previous design guidelines lead to a RCW with 16 corrugations with dimensions: d_c=5.88 mm, s_c=4.21 mm and t_c=0.8 mm (note that $\varepsilon_r = 1$ in our case).

Fig. 2 shows the dispersion diagram of the RCW computed with Ansys HFSS [11]. This plot only highlights two RCW modes, namely, mode HE_{11}, which pattern is shown in Fig. 3 (a), with a cut-off frequency of 4.24 GHz, and mode TE_{12}, shown in Fig. 3 (b), with a cut-off frequency of 13.42 GHz (notation is given in agreement with an equivalent circular waveguide [12]). Modes in light gray are orthogonal RCW modes that are barely excited by the CW of the final antenna. Conversely, mode TE_{12} can effectively be excited by the CW and, consequently, the cut-off frequency of this mode sets the upper operating frequency of the antenna.
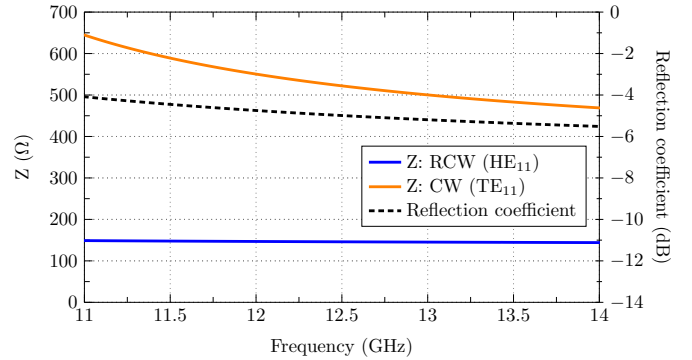

Fig. 4. Fundamental modes of the radially corrugated waveguide (RCW) and the circular waveguide (CW): real part of the impedance (Z), and reflection coefficient.

III. RADIALLY CORRUGATED HORN ANTENNA

Fig. 3 (a) shows how mode HE_{11} spreads across the whole inner area of the RCW with a uniform amplitude, thereby producing a large aperture efficiency when the RCW is opened to the free space. In order to excite this mode, the RCW is fed by a CW with diameter D_w=19.35 mm, whose fundamental mode (TE_{11}) has a cut-off frequency of 9.18 GHz (see Fig. 2).

The direct feeding of the RCW with a CW would produce a great reflection due to the impedance mismatch between mode HE_{11} in the RCW and mode TE_{11} in the CW, as shown in Fig. 4. This impedance mismatch is compensated by introducing two matching elements in the transition between the CW and the RCW, as depicted in Fig. 1. The first element is a circular metallic patch inside the CW, and the second element is a metallic ring on the transition plane. A foam layer is inserted between both elements to guarantee their correct separation. The circular patch acts as a capacitive element, whereas the metallic ring works as an inductance. The combination of both, in parallel and separated by a transmission line of length s, compensates the impedance mismatch shown in Fig. 4. Also, the insertion of the these elements helps to improve the axial symmetry and the cross-polar level of the radiation pattern.

By suitably optimizing the size and position of the matching elements, and the length of the corrugations (l_c), the return loss and the directivity at broadside can be maximized, and the side-lobe level (SLL) minimized. The optimized parameters, according to Fig. 1, are: d_p=7 mm, d_{ir}=3 mm, d_{or}=7 mm, t_p=0.7 mm, t_r=0.1 mm, s=4.4 mm, and l_c=6.93 mm.

Fig. 5 (a) shows the electric field on the aperture of the optimized RCHA. As can be observed, the field distribution is nearly uniform and linearly polarized, quite similar to mode HE_{11} pattern.

IV. PROTOTYPE AND MEASUREMENTS

The designed RCHA has been fabricated for validation purposes by a milling process that provides a surface roughness lower than 2 μm and a mechanical tolerance better than 30 μm. Fig. 6 shows two pictures of the prototype where, as can be observed, the metallic ring is located on the upper face of a foam layer to guarantee the air gap between the circular
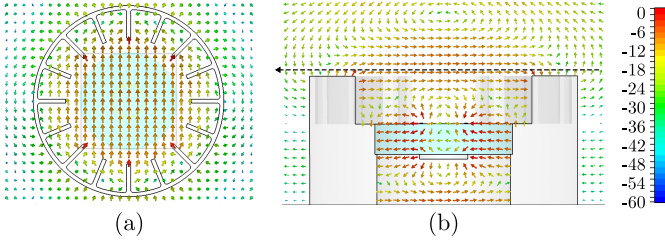
Fig. 5. Electric field in the structure at 13 GHz: (a) E-field on the aperture, and (b) E-field along the structure.

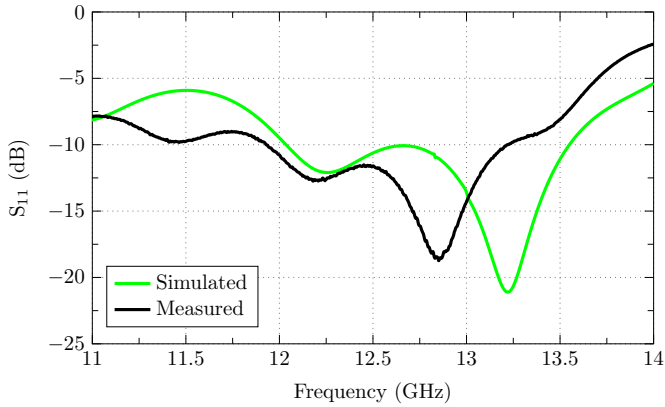Fig. 6. Pictures of the fabricated radially corrugated horn antenna: (a) 3D view, and (b) upper view (RCW).

Fig. 7. Measured S_{11} parameter of the radially corrugated horn antenna.

patch (inside the waveguide) and the ring. A total of eight holes have been drilled in the foam layer to minimize the equivalent permittivity of this layer. Note that, for the ease of manufacturing, a straight outer aluminum piece has been manufactured. Inside this metallic structure, the feeding CW has the same dimensions as those shown in Fig. 1 (b). Measurements have been performed using a rectangular to circular waveguide transition (not shown in the pictures) to permit the characterization with common rectangular waveguide flanges.

The S_{11} parameter of the RCHA, plotted in Fig. 7, shows an acceptable level ($S_{11} < -10$ dB) within the operating frequency band 11.93-13.22 GHz, which means a relative bandwidth of 10.25%. The discrepancy between measured and simulated results is produced by the non-perfect simulation of the rectangular to circular waveguide transition. Note that the narrow bandwidth is caused by the use of a metamaterial (corrugations) on lateral walls, which resonates at the given central frequency with a narrow bandwidth.
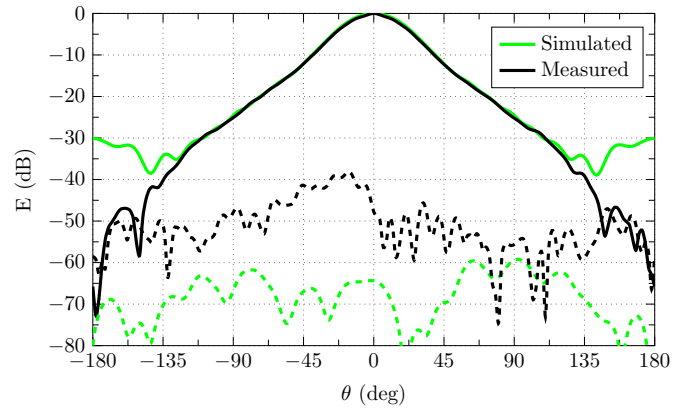

Fig. 8. Measured H-plane radiation pattern of the fabricated radially corrugated horn antenna at 13 GHz. Solid lines are the co-polar component, and dashed lines are the cross-polar component.
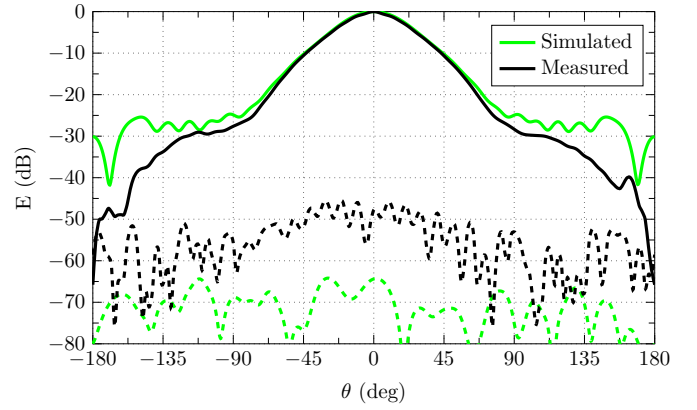

Fig. 9. Measured E-plane radiation pattern of the fabricated radially corrugated horn antenna at 13 GHz. Solid lines are the co-polar component, and dashed lines are the cross-polar component.

Fig. 10. Measured radiation pattern at $\phi = 45°$ of the fabricated radially corrugated horn antenna at 13 GHz. Solid lines are the co-polar component, and dashed lines are the cross-polar component.
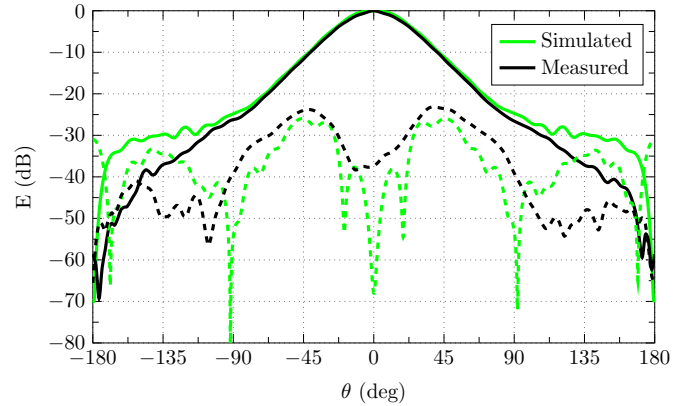
Figs. 8, 9, and 10 compare the measured and simulated radiation pattern on main planes. As can be observed, the SLL is below -26 dB in all planes. The co-polar pattern is rotationally symmetric, which is a common requirement in feeders of communication satellites to create circular spots on Earth, and the cross-polar component is below -25 dB.

TABLE I
COMPARISON OF MAIN RESULTS WITH PREVIOUSLY PUBLISHED WORKS.

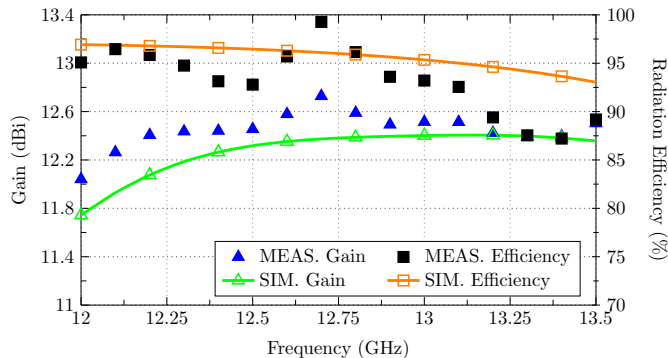| Horn antennas	Length (λ)	SLL	Crosspolar	Ap. Efficiency
Hard horn [5]	19.43	-18.0 dB	-30.0 dB	88.0%
Potter horn [6]	2.20	-27.0 dB	-32.0 dB	74.0%
Corrugated horn [7]	8.05	-23.0 dB	-35.0 dB	60.2%
Dielectric loaded horn [13]	8.10	-19.0 dB	-40.0 dB	90.0%
RCHA (This work)	**0.30**	-25.7 dB	-25.0 dB	72.0%

Fig. 11. Maximum gain and radiation efficiency of the proposed radially corrugated horn antenna vs. frequency.

The maximum gain and the radiation efficiency of the RCHA are presented in Fig. 11. As can be observed, the maximum gain is above 12.2 dBi at almost all frequencies, and the radiation efficiency is above 85%. Losses are caused by the metallic walls (made of aluminum) and the foam layer between the metallic ring and the patch. Note that, at some frequency points, the measured gain is higher than the simulation while the measured efficiency is lower than the simulation because the measured losses present a larger variation than the simulated ones. The large extension of the electric field on the aperture of the RCHA (see Fig. 5 (a)) gives an aperture efficiency above 72% at any frequency.

Table I shows a comparison between the main parameters of the proposed antenna and those of several previous works. As can be observed, the RCHA presents a considerably high aperture efficiency, comparable to those of other works, with a good cross-polar level, and with a length several times shorter than any of previous proposals. This low profile characteristic causes an appealing reduction of weight and volume in feeds for space applications.

V. CONCLUSIONS

This letter proposes a low-profile horn antenna formed by a circular waveguide with radial corrugations opened to the free space region. To minimize the cross-polar level and maximize the aperture efficiency, mode HE_{11} is excited in the corrugated waveguide by means of a circular waveguide. Two matching elements are inserted in the interface between both waveguides to improve the return loss level and minimize the excitation of orthogonal modes in the corrugated waveguide.

Measured results of a fabricated prototype show a return loss bandwidth of 10.25% (note that satellite communication systems normally demand less than 10%), and a rotationally-symmetric radiation pattern with a cross-polar level below -25 dB. The aperture efficiency of the antenna is better than 72%, and the radiation efficiency is above 85% within the operating frequency band. This good performance is obtained with a length of the structure of just l_c=6.93 mm, i.e., 0.3λ. This low profile entails a save of mass and weight that makes the proposed RCHA an ideal feed for communication satellites.

REFERENCES

[1] S. K. Rao, "Parametric design and analysis of multiple-beam reflector antennas for satellite communications," *IEEE Antennas and Propagation Magazine*, vol. 45, no. 4, pp. 26–34, 2003.

[2] ——, "Advanced antenna technologies for satellite communications payloads," *IEEE Transactions on Antennas and Propagation*, vol. 63, no. 4, pp. 1205–1217, 2015.

[3] A. K. Bhattacharyya and G. Goyette, "A novel horn radiator with high aperture efficiency and low cross-polarization and applications in arrays and multibeam reflector antennas," *IEEE Transactions on Antennas and Propagation*, vol. 52, no. 11, pp. 2850–2859, 2004.

[4] Q. Wu, C. P. Scarborough, D. H. Werner, E. Lier, and R. K. Shaw, "Inhomogeneous metasurfaces with engineered dispersion for broadband hybrid-mode horn antennas," *IEEE Transactions on Antennas and Propagation*, vol. 61, no. 10, pp. 4947–4956, 2013.

[5] O. Sotoudeh, P.-S. Kildal, P. Ingvarson, and S. P. Skobelev, "Single-and dual-band multimode hard horn antennas with partly corrugated walls," *IEEE Transactions on Antennas and Propagation*, vol. 54, no. 2, pp. 330–339, 2006.

[6] P. D. Potter, *A new horn antenna with suppressed sidelobes and equal bandwidths*. Jet Propulsion Laboratory, California Institute of Technology, 1963.

[7] J. Teniente, A. Martínez, B. Larumbe, A. Ibáñez, and R. Gonzalo, "Design guidelines of horn antennas that combine horizontal and vertical corrugations for satellite communications," *IEEE Transactions on Antennas and Propagation*, vol. 63, no. 4, pp. 1314–1323, 2015.

[8] H. C. Moy-Li, M. Ferrando-Bataller, D. Sanchez-Escuderos, and M. Baquero-Escudero, "Low-profile circularly-simmetric antenna with radial corrugations," in *2015 IEEE International Symposium on Antennas and Propagation*, 2015, pp. 2083–2084.

[9] G. L. James and B. M. Thomas, "TE_{11} to HE_{11} cylindrical waveguide mode converters using ring-loaded slots," *IEEE Transactions on Microwave Theory and Techniques*, vol. 30, no. 3, pp. 278–285, 1982.

[10] P.-S. Kildal, "Artificially soft and hard surfaces in electromagnetics," *IEEE Transactions on Antennas and Propagation*, vol. 38, no. 10, pp. 1537–1544, 1990.

[11] Ansys Corporation, "HFSS (high frequency structural simulator)," 2014, Suite v15, Pittsburg (PA), USA.

[12] C. Lee, S. Lee, and S. Chuang, "Plot of modal field distribution in rectangular and circular waveguides," *IEEE transactions on microwave theory and techniques*, vol. 33, no. 3, pp. 271–274, 1985.

[13] E. Lier and A. Kishk, "A new class of dielectric-loaded hybrid-mode horn antennas with selective gain: Design and analysis by single mode model and method of moments," *IEEE Transactions on Antennas and Propagation*, vol. 53, no. 1, pp. 125–138, 2005.